



Kent Academic Repository

Chuprin, Andrei D., Batchelor, John C. and Parker, Edward A. (2001) *Design of Convolved Wire Antennas using a Genetic Algorithm*. IEE Proceedings: Microwaves, Antennas and Propagation, 148 (5). pp. 323-326.

Downloaded from

<https://kar.kent.ac.uk/426/> The University of Kent's Academic Repository KAR

The version of record is available from

<https://doi.org/10.1049/ip-map:20010648>

This document version

Author's Accepted Manuscript

DOI for this version

Licence for this version

UNSPECIFIED

Additional information

Versions of research works

Versions of Record

If this version is the version of record, it is the same as the published version available on the publisher's web site. Cite as the published version.

Author Accepted Manuscripts

If this document is identified as the Author Accepted Manuscript it is the version after peer review but before type setting, copy editing or publisher branding. Cite as Surname, Initial. (Year) 'Title of article'. To be published in *Title of Journal*, Volume and issue numbers [peer-reviewed accepted version]. Available at: DOI or URL (Accessed: date).

Enquiries

If you have questions about this document contact ResearchSupport@kent.ac.uk. Please include the URL of the record in KAR. If you believe that your, or a third party's rights have been compromised through this document please see our [Take Down policy](https://www.kent.ac.uk/guides/kar-the-kent-academic-repository#policies) (available from <https://www.kent.ac.uk/guides/kar-the-kent-academic-repository#policies>).

Design of Convolved Wire Antennas Using A Genetic Algorithm

A.D. Chuprin, J.C. Batchelor and E.A. Parker

This paper is a postprint of a paper submitted to and accepted for publication in IET Microwaves, Antennas and Propagation and is subject to Institution of Engineering and Technology Copyright. The copy of record is available at IET Digital Library

Design of Convolved Wire Antennas Using A Genetic Algorithm

A.D. Chuprin, J.C. Batchelor and E.A. Parker

Abstract: The Genetic Algorithm technique has been used to optimize the design of small folded wire antennas. The genetic optimizer located wires on a predefined grid to create well matched devices operating at single or multiple bands. The chromosome structure and the fitness function employed are described. The GA approach also enabled broadband radiators and electrically small convoluted geometries to be designed.

1 Introduction

Genetic optimization has been applied to electromagnetic problems with significant success over the last 10 years. Notable applications have been in multi-layer absorber design [1], Frequency Selective Surfaces [2,3], Yagi array optimization, [4] and to printed patch design [5]. Genetic Algorithms (GAs) are suited to the optimization of electromagnetic structures as they cope well with multiple input parameter design tasks. They are also able to solve for different independent and loosely related goals simultaneously. Their stochastic nature gives good global search properties, reducing the local minimum problem often associated with Gradient type and other deterministic optimizers. A common criticism of GAs is the amount of intuition required and uncertainty involved in the selection of the optimizer control parameters, such as population size and probability and type of cross-over used. While it is true that some experience is usually required to solve a non-trivial problem successfully by GA, it must also be stated that the simplicity and flexible application of the process often outweighs the uncertainty in the control settings. Commonly available GA optimizers often include preset values (e.g. probability of mutation) which give acceptable solutions in the first instance. Empirical guidelines have been reported in the literature, though these are often problem dependent and vary according to the implementation of the GA. Research into knowledge based GAs continues to address these issues [6]. This paper describes the use of a GA to design printed wire structures by selection of wires from a predefined grid. **The following design goals are addressed in each section:** input matching at single and multiple frequencies,

frequency minimization, broadband operation, radiation pattern shape, and the removal of low current carrying wires in the final structure.

2 Wire grid structure

All the printed antennas described in this paper have been derived from a predefined rectangular grid of wires, as depicted in Fig.1. The grid had total side lengths of L_x and L_y , each side consisting of N_x and N_y joined wires in the x and y directions respectively. All the gridlines were in the same plane and equally spaced, thus forming a lattice of $N_x \times N_y$ simple rectangular cells of dimensions l_x and l_y given by (1):

$$l_{x,y} = \frac{L_{x,y}}{N_{x,y}}. \quad (1)$$

The planar nature of the grid meant that all wires were joined at their end points. The individual wires were normally much less than one wavelength in length and could be further segmented for basis current representation in an electromagnetic solver using the method of moments technique. The grid structure used in this study had the parameters, $N_x = N_y = 10$, which gave the total number of wires $N_t = 10 \times 11 \times 2 = 220$. The wires were electrically thin with a constant radius of 1mm. There was no ground plane or dielectric substrate present. A balanced feed point was modelled by impressing a voltage across one of the wires.

The genetic optimizer produced antennas from the grid by selecting individual wires to be present. All the genetic structures were subsets of the full grid and each had a total number of wires N_w . N_w varied according to each specific structure and was always less than or equal to N_t .

3 Chromosome Representation

The grid structure formulated above was represented by a binary chromosome. The basic chromosome string consisted of 3 parts and was of total length $N_t + N_{ex} + N_s$. It had the following form:

$$\overbrace{101100010010110\dots}^{N_t} \overbrace{1101\dots}^{N_{ex}} \overbrace{01}^{N_s}$$

where N_t was the total number of wire locations in the grid (220). The presence or absence of each wire was represented by 1 or 0 in the first N_t bits. The digit 1 occurred N_w times in the first N_t bits. The excited wire number, m , was coded in the next N_{ex} bits, and the feed was set to be the wire represented by the m^{th} 1 in the N_t string. If in the operation of the routine the value of m chosen was greater than N_w , then N_w was subtracted from m until this was not the case. Finally, the excited segment of the feed wire was represented by N_s bits, which indicated the segment of the feed that was to have a voltage impressed across it. The short electrical length of the individual grid wires allowed N_s to be set at 1 segment for most cases.

The structures were modelled with NEC-2 [7] which solves current distributions on metal wire structures using the method of moments. NEC models filamental wires which can represent very thin strips of metal. According to Popovic, the strip width is four times the wire radius, [8]. NEC-2 was interfaced with a GA solver called PGAPack [9].

4 Input matching

4.1 Single frequency matching formulation

The genetic optimizer was initially set the design task of evolving structures with inputs matched to 50Ω at a single specified frequency (1.8GHz). The grid side lengths L_x and L_y were set equal to 8.3cm which was one half wavelength at the design frequency. The fitness (or cost) function was specified to be of the form

$$Fitness = w_1 \times |Z_{in} - 50| + w_2 \times \sum_{\theta=0}^{2\pi} |P_{\theta} - P_{max}| + w_3 N_w \quad (2)$$

where Z_{in} is the input impedance in ohms computed by the solver, P_{θ} is the radiated power at angle θ , and P_{max} is the maximum power radiated at a single angle within the plane of interest. The coefficients w_1 , w_2 and w_3 are weighting factors to prevent individual terms in the fitness function from dominating others. The second term of the fitness function is necessary to avoid the case of well matched resonant structures with poor radiation efficiencies in the plane of interest, or with unphysical superdirective gains. The final term in (2) can be used to minimize the number of individual wires in the final solution.

4.2 Single frequency matching results

The GA was set to run with a total replacement of the parent population, keeping only the single best, elite, solution. A comparison was made where the optimizer was allowed to design structures with no constraint on the numbers of wires present against the case where a limit was placed on N_w . With $w_3 = 0$ in (2) the optimizer was able to achieve fitness approaching zero for single frequency impedance matching and it became apparent that many comparable local minima existed, each satisfying the fitness criteria. A typical example of a single frequency matched structure with no limit on wire number is shown in Fig.2a. The design is clearly complex and an investigation of the current magnitude flowing on the structure revealed that many wires did not carry significant currents. Setting $w_3 \neq 0$ reduced the complexity of the optimal structures. It was necessary to select weighting factors to prevent the optimizer favouring solutions with zero wires present. The exact value of the weighting coefficients was not essential, though a good choice involved ensuring that the individual fitness function terms would be of the same order of magnitude for solutions close to the optimum. With this additional constraint a significant reduction in the number of structure wires was observed, with N_w falling from typical values of about 120 to around 60. A reduced wire solution is illustrated in Fig.2b. The number of isolated wires falls from 7 in Fig.2a to just 2 in Fig.2b. Inspection of a large set of solutions indicated that with the number of wires minimized, structures took on the general form of 1 to 3 folded halfwave dipoles carrying sinusoidal current distributions. The fact that different solutions were obtained for each GA run demonstrated that the constraints applied did not locate a single dominant global

solution. Many comparable local solutions were produced which satisfied the cost function, and therefore more precise specification of the radiation pattern could help to differentiate between local optima and a unique global solution.

4.3 Multi-frequency input matching

The fitness function for multiple frequency input matching took the form:

$$fitness = \sum_{n=1}^N |Z_n - 50| \quad (3)$$

where Z_n was the input impedance at frequency f_n . A solution for $N = 3$ is illustrated in Fig.3 which shows the frequency dependence of the return loss for the inset antenna structure. The frequency points specified were 1600, 2000 and 2400MHz. Return losses of better than 10dB were achieved in each case, but it should also be noted that between the first two matches S_{11} never rose above -10 dB. If good isolation is required between the various operating bands, frequency points could be specified where the return loss is required to approach 0dB. The total boresight gain for the structure of Fig.3 was calculated to drop by 6dB between the upper and lower bands, which was a consequence of the main beam shifting from boresight to 50° elevation. This was because boresight radiation was not included as a constraint in the fitness function. The structure was excited by a single source, though designs could be developed with independently fed separate bands if required. The fitness function would then be required to reward isolation between the feeds for the various bands. The optimizer was capable of running with up to 6 separate and independently matched frequency points ($N = 6$).

4.4 Broadband matching

The multiple frequency point matching approach described in section 4.3 was adapted to provide a method for broad band design, by requiring that the points should be close together in frequency. Stipulating that matching should be optimized at 900, 1000, 1100 and 1200 MHz resulted in the return loss shown in Fig.4. The antenna was matched over a $S_{11} \leq 10$ dB bandwidth of 35% where the total side length of the

grid was a half wavelength at the band centre. The total gain at boresight fell by 3.5dB over this band. Comparable halfwave dipole bandwidths are in the region of 20%.

5 Frequency minimization

Personal communication systems require reduced size antennas, where the tendency is to approach the Hertzian dipole characteristics of reactive input impedance, dipole radiation patterns and very limited bandwidths. The optimizer was set the task of reducing the operating frequency of a grid based antenna with fixed side length 8cm and wire radius 1mm. This was implemented by adding the simulation frequency to the fitness function which is minimized by the nature of the optimizer. Other terms in the fitness function required a close match to 50Ω and a maximized average gain. Results showed that input matched antennas could be derived which were only 20% of the length of a halfwave dipole, though this was associated with a fall in the -10dB S_{11} bandwidth to about 5%. Figure 5 shows the return loss plot for a reduced size antenna, with side length d of 7.5cm. The antenna structure is inset. The operating frequency was 600MHz, i.e. an operating wavelength λ_0 of 50cm. This represents a figure of merit of about 6.7, where the figure of merit is defined as $\frac{\lambda_0}{d}$, [10,11]. NEC calculated the boresight gain of this antenna to be about 1.7dBi which, as expected, is equal to that of a Hertzian dipole. Figure 6 shows a predicted radiation pattern for the structure in Fig.5 which confirms that it is equivalent to a Hertzian dipole. The reduced size antenna described here is matched over a 5% bandwidth, while a Hertzian dipole would require a matching circuit and would be an inefficient radiator.

6 Conclusions

The integration of a genetic search engine with an electromagnetic solver has been used to demonstrate the successful generation of various grid based antenna structures suitable for printing on planar surfaces. Impedance matching can be achieved at single or multiple frequency points using this technique, though control of the power gain must also be maintained to produce efficient radiators. The structures produced by the genetic optimizer often include many wires that do not carry significant currents, but the complexity can be reduced by including the number of wires in the structure as a parameter to be minimized. This process provided valuable insight into how the final structures related to their radiation patterns. However, no single unique

solution was discovered, suggesting that the search space must be reduced. It should be possible to design multiple band convoluted antennas with separate feed points for each band. Finally, it was shown that Hertzian size convoluted antennas can be produced with bandwidths acceptable for communications channels. All the structures were modelled in free space with no dielectric sheet or ground plane. This reduced solution times, but more practical designs will be result from substrate inclusion. Again future work should address these issues and also present a possibility for accurate practical validation of computed results.

7 Acknowledgement

This work was supported by a research grant from the UK Engineering and Physical Sciences Research Council.

References

- 1 Weile, DS., Michielssen, E. and Goldberg, DE.: 'Genetic Algorithm Design of Pareto Optimal Broadband Microwave Absorbers', IEEE Trans. Electromag. Compat., 1996, 38, (3), pp.518-525.
- 2 Manara, G., Monorchio, A. and Mittra, R 'Frequency selective surface design based on genetic algorithm', IEE Electron. Letts., 35, (17), 1999, pp.1400-1401.
- 3 Chuprin, AD., Parker, EA. and Batchelor, JC.: 'Convolute Double Square: Single Layer FSS with Close Band Spacings', IEE Electron. Letts., 2000, 36, (22), pp.1830-1831.
- 4 Altshuler, EE. and Linden, DS.: 'Wire-Antenna Designs Using Genetic Algorithms', IEEE Antennas and Propagation Magazine, 1997, 39, (2), pp.33-43.
- 5 Johnson, JM. and Rahmat-Samii, Y.: 'Genetic Algorithms and Method of Moments (GA/MOM) for the Design of Integrated Antennas', IEEE Trans. Antennas Propagat., 1999, 47, (10), pp.1606-1614.
- 6 Muscat, A.F. and Parini, CG.: 'Design of Novel Microstrip Antenna Structures Using Knowledge Intensive CAD', Proc. AP-2000, Davos, April 2000, p.470.
- 7 Burke, G.J. and Poggio, A.J.: 'Numerical Electromagnetics Code Method of Moments', Lawrence Livermore Lab, US, 1981.
- 8 Popovic, B.D. and Kolundzija, B.M.: 'Analysis of metallic antennas and scatterers', IEE Publishing, ISBN 0 85296 807 8.
- 9 Levine, D.: 'Users Guide to the PGAPACK Parallel Genetic Algorithm Library', Tech. Rep. ANL-95/18, Argonne National Laboratory, 1995.
<ftp.mcs.anl.gov>.
- 10 Parker, E.A. and El Sheik, A.N.A.: 'Convolute Array Elements and Reduced Size Unit Cells for Frequency Selective Surfaces', IEE Proc. H. Microw. Antennas Propag., 1991, 138, pp.19-22.
- 11 Chuprin, A.D., Parker, E.A. and Batchelor, J.C.: 'Resonant Frequencies of Open and Closed Loop Frequency Selective Surface Arrays', IEE Electron. Letts., 2000, 36, (19), pp.1601-1603.

Figure captions:

Figure 1:

Rectangular grid basis for genetically derived antennas.

Figure 2:

Convolved antenna structures produced by genetic search

—■— Feed point

(a) Total wire number unconstrained (b) Wire number minimized by search

Figure 3:

Return loss of triple band convoluted antenna structure.

Vertical axis: $|S_{11}|$ (dB), Horizontal axis: Frequency (MHz)

Figure 4:

Return loss for the inset multiband convoluted antenna structure.

Vertical axis: $|S_{11}|$ (dB), Horizontal axis: Frequency (MHz)

Figure 5:

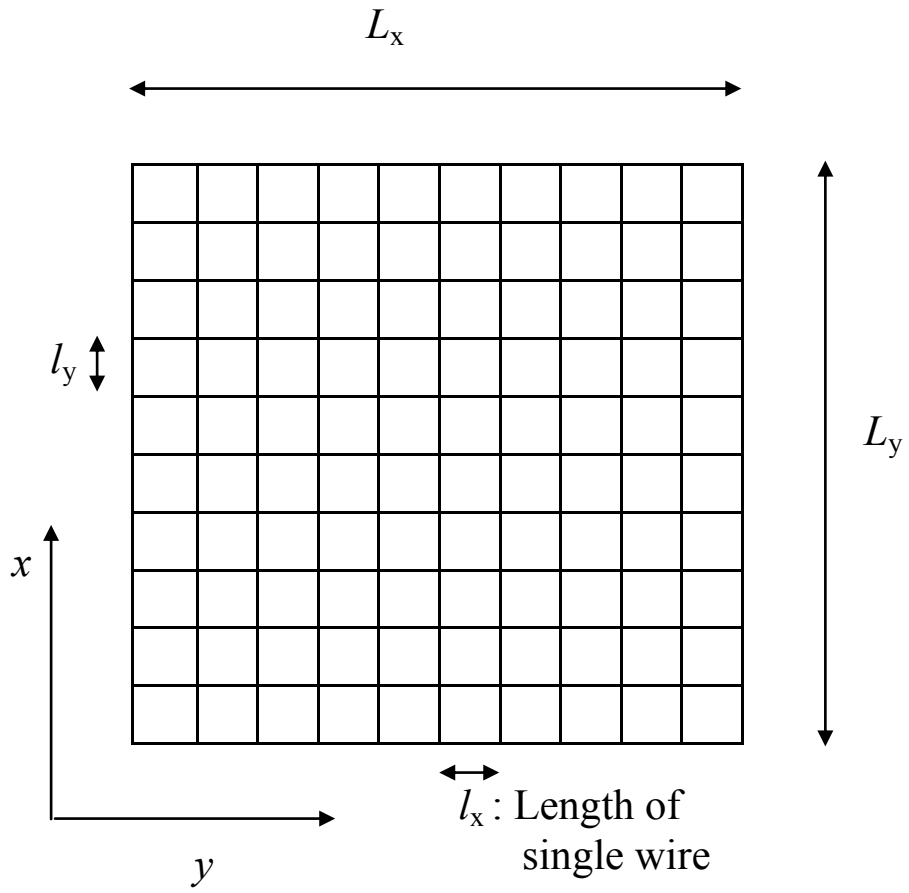
Return loss for the inset single band frequency reduced antenna structure.

Vertical axis: $|S_{11}|$ (dB), Horizontal axis: Frequency (MHz)

Figure 6:

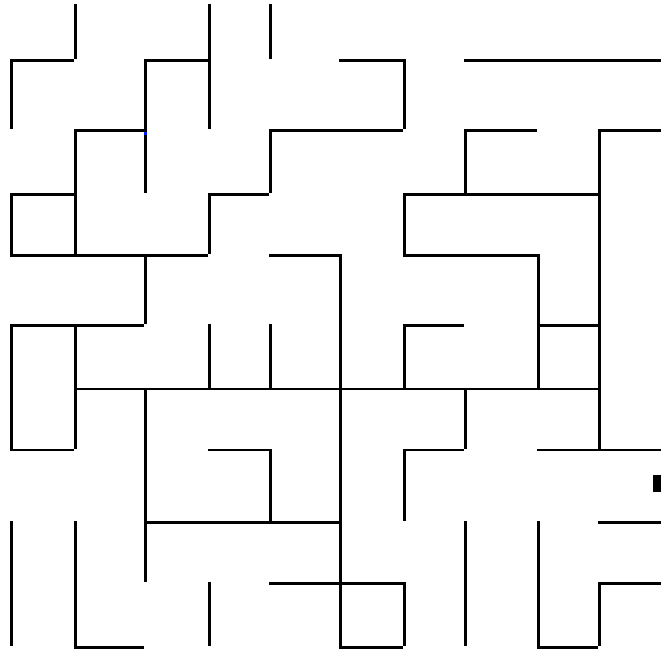
Co-polar radiation pattern in x - z plane for the reduced size antenna in Fig.5. (y - z plane pattern is identical).

Figure 1



Rectangular grid basis for genetically derived antennas.

Figure 2a

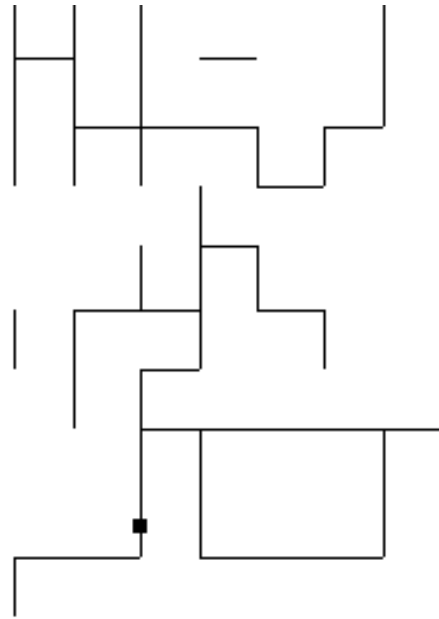


Convoluted antenna structures produced by genetic search

—■— Feed point

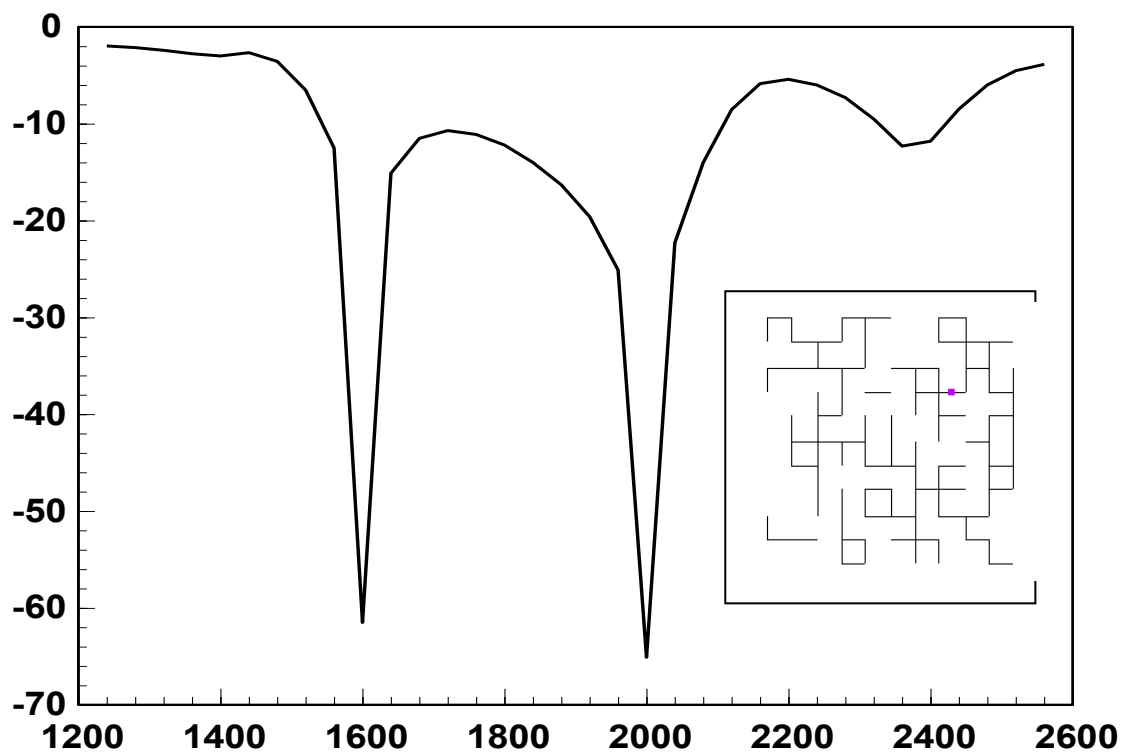
(a) Total wire number unconstrained

Figure 2b



(b) Wire number minimized by search

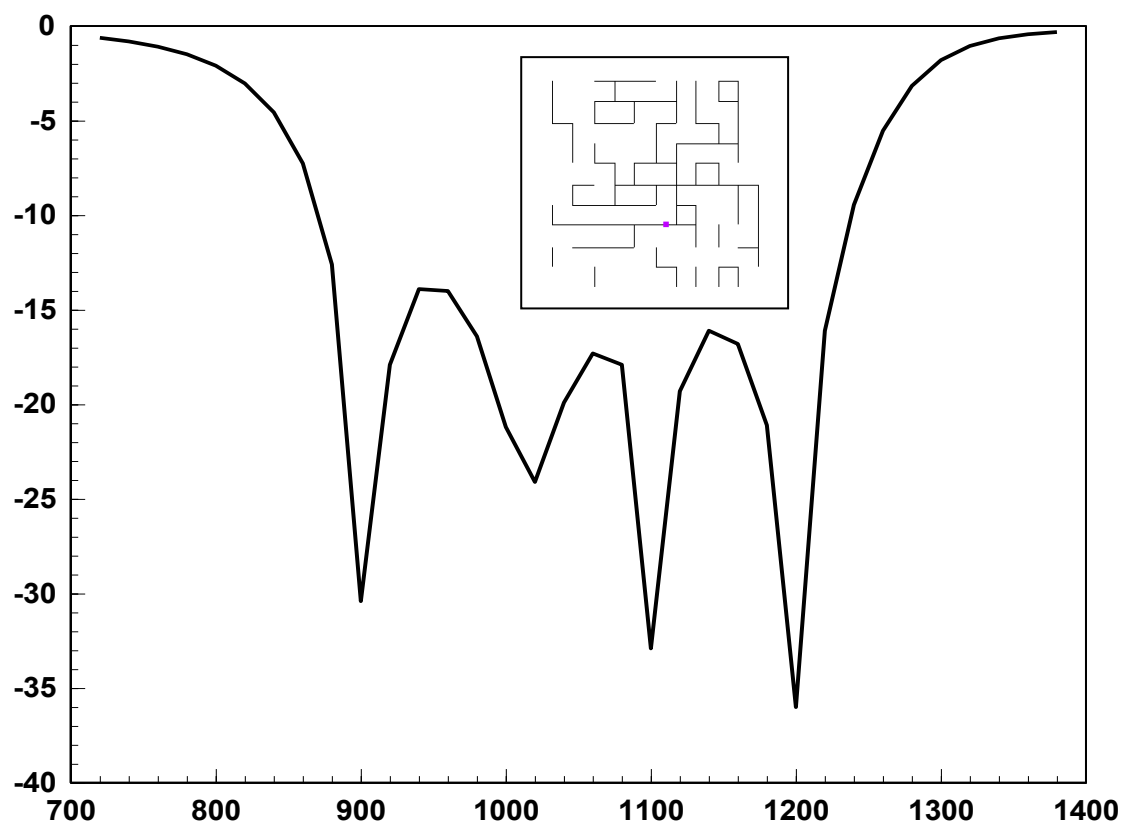
Figure 3



Return loss of triple band convoluted antenna structure.

Vertical axis: $|S_{11}|$, Horizontal axis: Frequency (MHz)

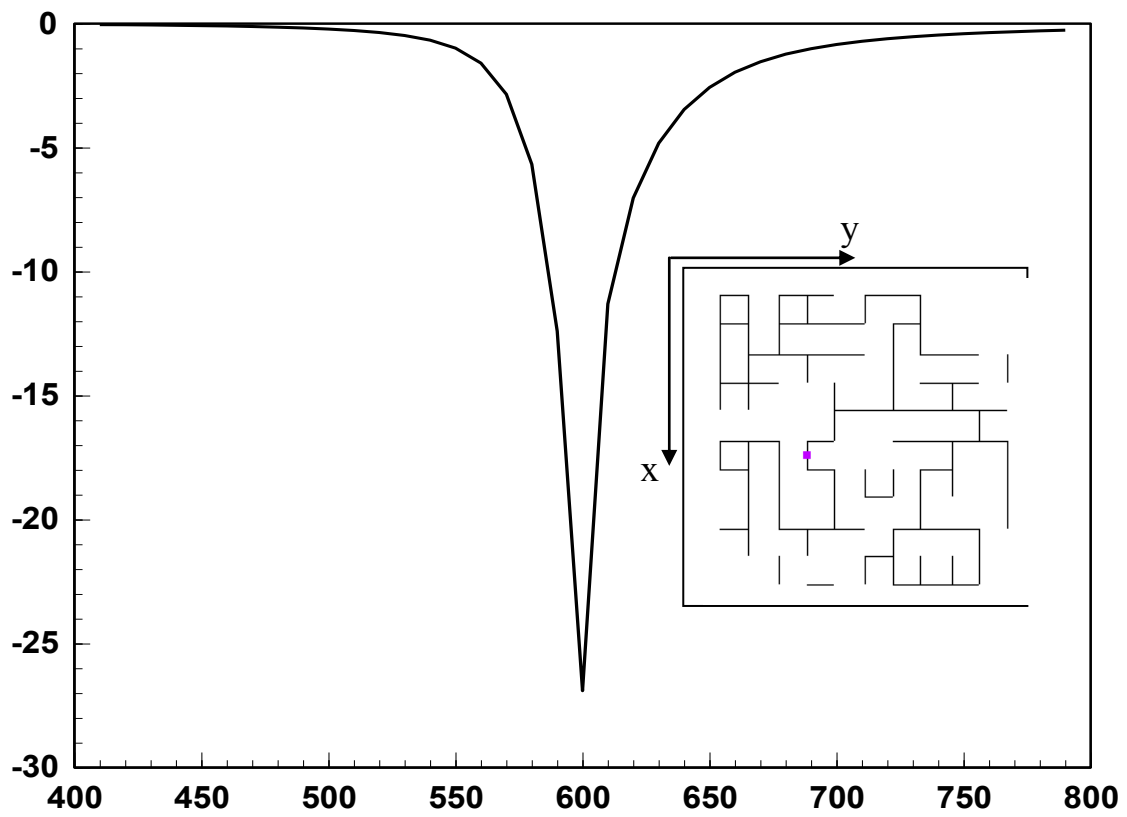
Figure 4



Return loss for the inset multiband convoluted antenna structure.

Vertical axis: $|S_{11}|$, Horizontal axis: Frequency (MHz)

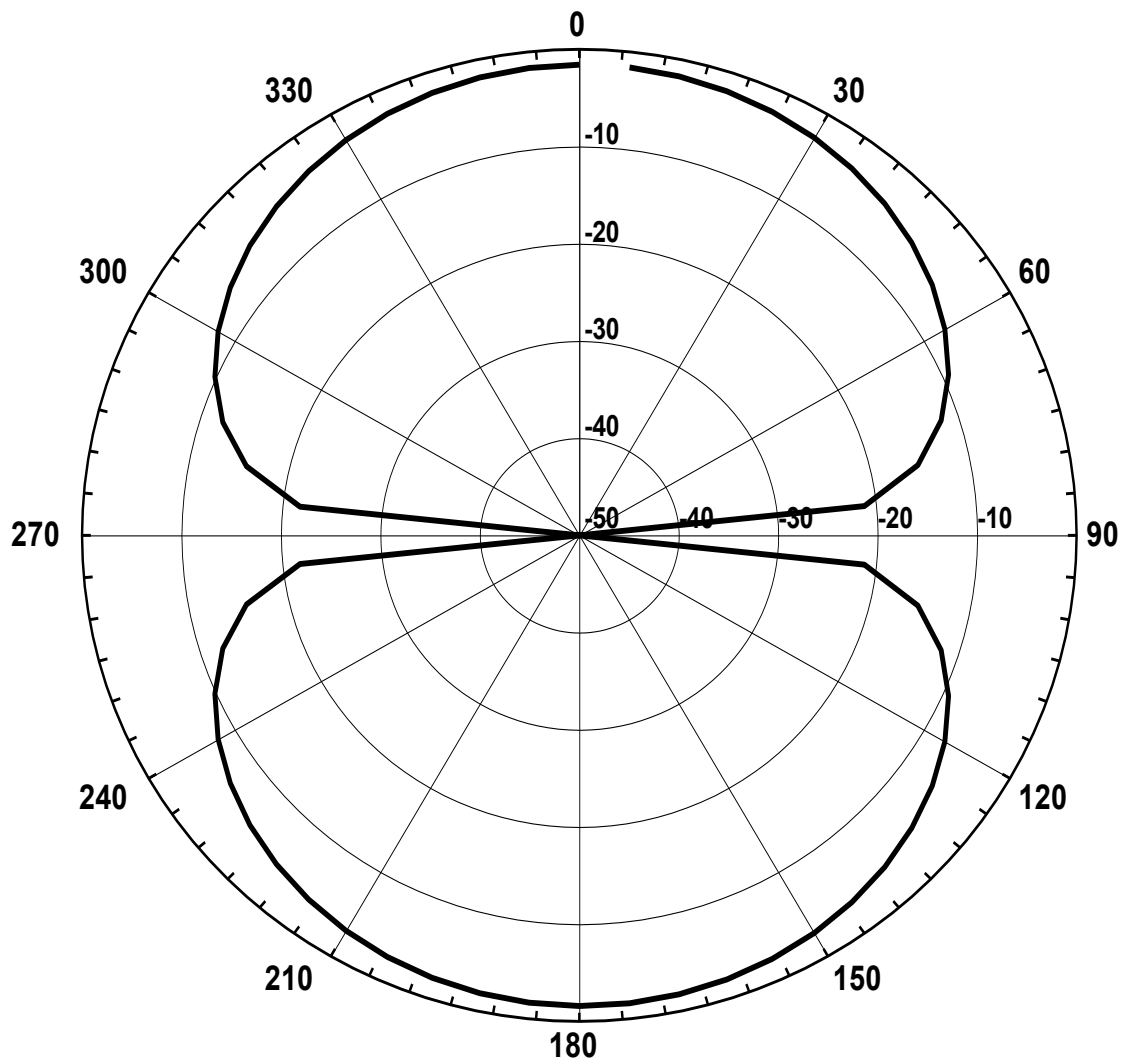
Figure 5



Return loss for the inset single band frequency reduced antenna structure.

Vertical axis: $|S_{11}|$, Horizontal axis: Frequency (MHz)

Figure 6



Vertically polarized radiation pattern in x - z plane for the reduced size antenna in Fig.5. (y - z plane pattern is identical).